

Mechanochemical activation of minerals on the cordierite synthesis

S. Tamborenea^{a,1}, A.D. Mazzoni^{a,b,*}, E.F. Aglietti^{a,b}

^a Centro de Tecnología de Recursos Minerales y Cerámica (CETMIC), C no. Centenario y 506-CC49 (1897) M.B. Gonnat, Bs.As, Argentina

^b CONICET UNLP, La Plata, Argentina

Received 6 May 2003; received in revised form 16 August 2003; accepted 27 August 2003

Abstract

The cordierite is commonly prepared by reaction of talc, clay and gibbsite within the range of 1200–1350 °C. This study deals with the effect of the amorphization by grinding of that mixture and its influence on the cordierite formation.

The mixture previously mentioned underwent six different treatments: mixing without grinding (A) (only mixing); non-amorphizing grinding (A_M) and amorphizing grinding in oscillating mill at four different times (H samples). The phases formed by thermal treatment were studied using differential thermal analysis (DTA)–thermogravimetric analysis (TG)–DTG, dilatometries and X-ray diffraction (XRD) techniques in certain combinations.

The thermal analysis of the A and A_M series were compared and they do not show significant differences, whereas the H samples present remarkable alterations in the DTA peaks as well as in the weight losses (TG). Thus, a great number of DTA peaks tend to decrease the temperature of the maximum and to lower the intensity as the amorphization time increases.

Calcination tests performed within the range 900–1200 °C show important differences in the diffractograms obtained from the intermediate products. While at 1350 °C the A and H samples reach the same final phases, within the range 1200–1360 °C they present important differences in the DTA indicating that the sequence and direction of reaction are different. The same behavior can be observed by dilatometric analysis.

© 2003 Elsevier B.V. All rights reserved.

Keywords: Cordierite; Mechanochemical; Processing; DTA–TG; Dilatometry

1. Introduction

Cordierite, whose composition is $2\text{MgO}\cdot 2\text{Al}_2\text{O}_3\cdot 5\text{SiO}_2$, is one of the phases of the $\text{MgO}\text{--}\text{SiO}_2\text{--}\text{Al}_2\text{O}_3$ system [1]. This compound is a ceramic material technologically applied in many fields due to its properties, such as its low thermal expansion coefficient that makes it suitable to tolerate sudden changes in temperature [2].

The most common method to obtain these phases is from mixtures of solid powders such as: talc, clays, gibbsite, alumina, magnesia, etc., submitted to under thermal treatments between 1250 and 1350 °C [3].

Different processes can remarkably influence the reactivity of the solids. Particularly, the mechanical treatments are important as long as they can help to produce changes in the texture and structure of the solids [4]. In many cases,

these alterations in the structure cause certain modifications in the phases formed by thermal treatment of the solids mechanochemically treated. Many works have been written about the influence of the mechanochemical treatments on many minerals and compounds.

Kaolinite [5–8], gibbsite [9] and talc [10] undergo important structural alterations when they are submitted to intensive grinding. The phases formed as a consequence of the mechanical treatment of mixtures of two or more precursors have recently been studied: kaolinite–gibbsite mixtures for the formation of mullite [11,12]; gibbsite–brucite mixtures where the spinel formation [13] and talc–clay–gibbsite mixtures for the formation of cordierite [14,15].

The influence of the mechanical treatment by grinding on the formation of cordierite from a talc, kaolinitic clay and gibbsite mixture is studied in this work.

2. Experimental methodology

The starting materials used were talc, kaolinitic clay and gibbsite, whose compositions are shown in Table 1. The

* Corresponding author. Tel.: +54-221-4840247; fax: +54-221-4710075.

E-mail addresses: mazzoni@cetmic.unlp.edu.ar, mazzoni@netverk.com.ar (A.D. Mazzoni).

¹ CICPBA fellowship.

Table 1
Chemical composition of the minerals (%)

Minerals	SiO ₂	Al ₂ O ₃	MgO	CaO	Fe ₂ O ₃	TiO ₂	K ₂ O + Na ₂ O	LOI
Talc	59.83	1.44	31.87	0.33	0.14	0.07	1.37	5.01
Clay	51.70	34.40	0.18	0.20	0.37	0.15	2.0	11.4
Gibbsite	0.05	64.10	0.0	0.0	0.0	0.0	0.60	34.20

kaolinitic clay presents a low content of quartz as impurity. They all had a particle size passing through mesh 325 ASTM ($d_{50} = 10\text{--}15\ \mu\text{m}$). The mixtures were made weighing the quantity of each mineral that generates by calcination the cordierite composition.

A Herzog HSM 100 oscillating mill, with a frequency of $12.5\ \text{s}^{-1}$ was used for grinding. This device works through friction and the impact caused by the relative movement of a ring and a concentric cylinder, placed within a casing containing the material to be ground. The mixtures (30 g) were milled in that mill for 5, 10, 15 and 20 min, and the samples were identified as H5, H10, H15 and H20, respectively.

The reference mixtures were A (without grinding, only mixing) and a mix named A_M treated in an attrition mill with alumina balls for 2 h at 400 rpm that does not produce mechanochemical effects during the treatment times employed.

Both mills do not produce contamination in the milling conditions employed in the present experiences.

The differential thermal analysis (DTA) and the thermogravimetric analysis (TG) were carried out with a Netzsch 409 equipment using platinum crucibles with $\alpha\text{-Al}_2\text{O}_3$ as reference and a heating rate of $5\ ^\circ\text{C}/\text{min}$.

The crystalline phases were determined by X-ray diffraction (XRD) with a Philips equipment using Cu K α radiation ($\lambda = 1.54\ \text{\AA}$). The particle size was determined with Sedi-graph equipment. Calcinations were carried out in furnace with air atmosphere.

BET specific surface area was measured with a Micromeritics Accusorb equipment.

Dilatometric curves were performed with a Netzsch dilatometer and a heating rate of $5\ ^\circ\text{C}/\text{min}$, on $25\ \text{mm} \times 8\ \text{mm} \times 8\ \text{mm}$ samples pressed at 100 MPa.

3. Results and discussion

The granulometric effect of the mixtures on the DTA–TG diagrams and XRD diffractograms was studied. The results obtained for the A samples (the thicker, $d_{50} = 10\ \mu\text{m}$) and those for A_M samples (the thinner $d_{50} = 1.5\ \mu\text{m}$) were compared. The results deduced from these diagrams (DTA–TG–XRD) are in agreement, therefore, the granulometric variations within the ranges used do not present significant effects under our conditions on the phenomena studied in this work. Only the A_M results will henceforth be described. Since the effects detected in H samples are

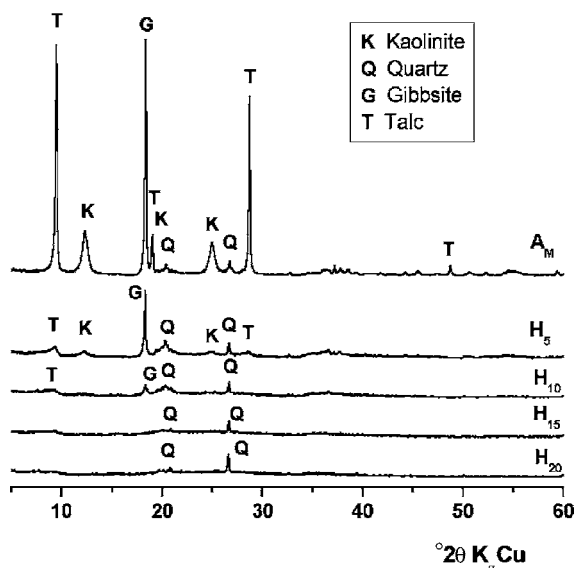


Fig. 1. XRD of the minerals mixtures before being calcined.

only due to the mechanochemical activation, they present d_{50} within the range of $4\text{--}6\ \mu\text{m}$ for the H5–H20 samples. This relatively high size is due to the binding effect caused by this mill, restraining the grinding process as regards the obtention of thinner sizes.

BET specific surface area shows an increase in the first 5 min of treatment and a sudden decrease at times longer than 10 min. The high surface areas attained suggest the creation of appreciable intraparticle porosity. H20 and A_M have similar surface areas. The samples treated in the Herzog mill had the same general behaviour.

The XRD of the H samples (Fig. 1) show an important decrease of the relative intensity of the peaks. The mineral mixture gradually loses crystallinity because of the grinding effect. At the beginning of the treatment this loss of crystallinity is greater. It must be taken into account that these compounds are relatively soft and according to previous studies the intensive grinding changes their texture and structure. It was not analyzed which of them underwent the greater structural damage. In spite of this the relative intensity of the peaks depend on the initial content of them in the mixture. For the H20 mixture, it was observed that the quartz peak was the only peak present since the grinding conditions could not affect it greatly because of its hardness and structure. It is logical that this effect continuously increases with the grinding time. The amorphization is important even in H5, reaching an almost complete destruction of the structure in H20 (observed by XRD).

The amorphization produces significant changes in the DTA–TG diagrams. The evolution of the diagrams as a function of grinding time from H5 to H20 is shown in Figs. 2–5. The A_M sample has well-defined DTA peaks. The first one is a strong endothermic peak at $327\ ^\circ\text{C}$ corresponding to the gibbsite dehydroxylation. This first peak gradually decreases in intensity and shifts to lower temperatures with increase of

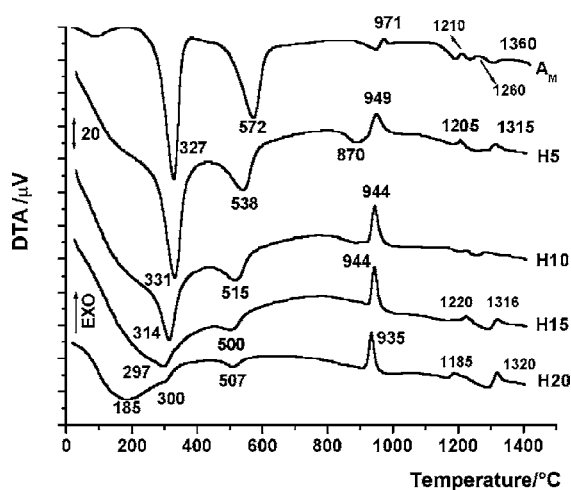


Fig. 2. DTA curves for the minerals mixtures.

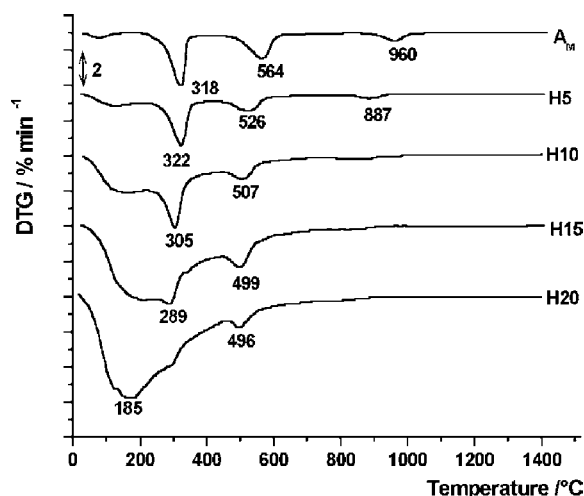


Fig. 5. DTG curves for the minerals mixtures.

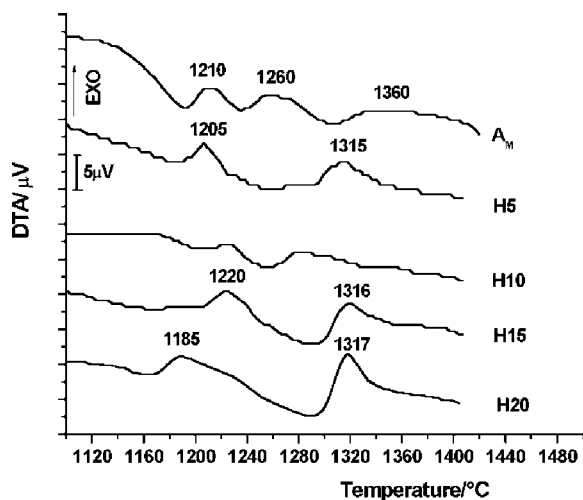


Fig. 3. DTA curves for the minerals mixtures between 1120 and 1400 °C.

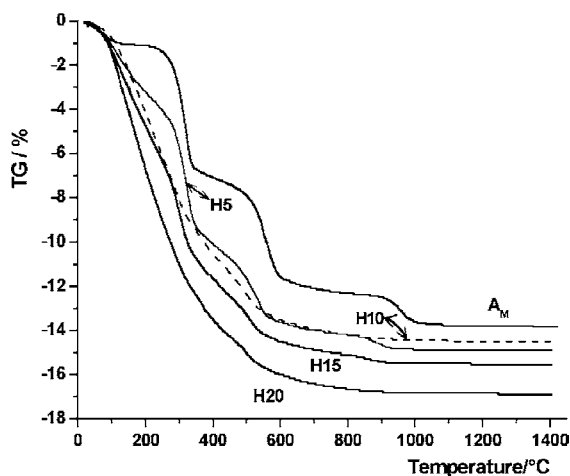


Fig. 4. TG curves for the minerals mixtures.

the grinding time, becoming in H20 almost imperceptible at near to 300 °C. Besides, this peak is gradually deformed by the presence of a shoulder in the low temperature side. This shoulder continuously increases up to be transformed into a centered band at 185 °C for the H20 sample. This broad endothermic band centered at about 185 °C, coming from the overlap of the dehydration of gibbsite and kaolinite [12], indicates the presence of hydroxyls slightly bounded to the original structure. This phenomenon is due to the energy accumulated by milling in the crystalline network that makes them less stable.

Some peaks that took place during the intermediate steps of the gibbsite dehydration were noticeable in the pure samples but not in the A_M ones due to the dilution effect. The study made on the pure sample about these peaks showed a behavior similar to the one described.

A second important endothermic peak is observed in A_M , centered at 572 °C, corresponding to the kaolinite dehydroxylation. This peak has a strong tendency to decrease its area and shifts to lower temperatures when milling. In H20, it became reduced to a small peak centered at 507 °C. A reduction of the temperature and of the peak area can be observed. This is due to the reduction of the energy necessary to destroy the crystalline structure of the system. The energy supplied by the oscillating mill causes structural disorder, through the distortion or breakage of the crystalline network. This is evident from the reduction of the intensities of XRD peaks. As kaolinite is a layer-structure mineral, impact or friction forces applied during comminution are resolved anisotropically according to crystallographic axis [8].

The A_M samples also present a small endothermic peak at 960 °C, corresponding to the talc dehydroxylation and its transformation to enstatite [5]. This is the only peak noticeable in well-crystallized talc samples. The samples mechanochemically treated showed a disordered phase whose decomposition is easier and took place at lower and not well-defined temperature compared to the original

ones. That endothermic peak appears in H5 near 870 °C with a smaller size indicating a smaller ΔH decomposition and it was not found in H10 where the structure has been destroyed.

Afterwards, a small exothermic effect at 971 °C appears in the mixture without treatment. This peak is due to the transformation of the non-crystalline structure of the kaolinite into a spinel or premullite phase. This peak moves to 949 °C in H5 reaching the 935 °C in H20. The size of this peak increases from H0 to H5 and then it has not important variations in the H5–H20 samples. The fact that the premullite phase does not appear as a crystalline phase using XRD must be taken into account.

H5–H20 samples appear to be more active with respect to subsequent thermal treatments, as the transformation of metakaolin to spinel (Si–Al–O) phase occurs at temperatures lower than A_M . Moreover, its reaction enthalpy (ΔH°) becomes smaller, as it is shown by the reductions in the exothermic peak area [6]. The DTA of cordierite glass with the same composition shows a peak at the same temperature. This peak appears as a shoulder of a great exothermic peak at 980 °C, which is associated to the formation of indialite that crystallizes from a non-crystalline glassy phase.

Within the range 1150–1380 °C (Fig. 3) a series of very weak thermal effects were detected ($<5 \mu V$). DeAza et al. [16] using a high sensitivity equipment found in talc–clay– CO_3Mg mixtures three exothermic peaks very weak at 1225, 1275 and 1357 °C, the first corresponding to the clay and the other two to the formation of cordierite [16]. In our case, the clay peak can be only detected in the A_M sample, whereas those corresponding to the cordierite formation can be observed in all the samples. In the H samples, the exothermic peak at 1350 °C shifts to temperatures of about 1315 °C, having a tendency to increase the height. The peak at 1275 °C also shifts to lower temperatures (~ 1180 °C for H20). DeAza et al. [16] also postulate an endothermic peak at 1330 °C associated with the formation of liquid phases. In our samples that peak is not clearly observed.

The analysis of the TG–DTG curves (Figs. 4 and 5) confirms the behaviors observed by DTA since the dehydroxylations are accompanied by the corresponding weight losses.

The A_M sample presents three mass loss steps well defined with DTG peaks at 318, 564 and 960 °C, which are in accordance with the three first DTA peaks described.

The grinding in the Herzog causes shifts (Fig. 5) in the DTG peaks to lower temperatures and size variations. The peaks at 318, 564 and 960 °C present a behavior similar to those of the DTA peaks at 327, 572 and 960 °C as they refer to the same phenomena. In correlation with this, the TG curves present three well-defined steps for A_M (Fig. 4), which became more diffused with the increase of the milling time, almost resulting in only one fall for H20. The TG curves show a slight increase of the total weight loss with the milling time. This phenomenon can be explained by the

fact that the samples absorbed greater amounts of water as the activation produced a surface increase.

Everything described up to now is consistent with the crystalline structure loss that takes place when the mechanical energy is transferred by means of milling. Thus, even though the chemical composition of the mixtures are the same, their different “crystallinity degree” and “accumulated energy” produce different behaviors during calcinations between 20 and 1200 °C.

The XRD analyses during the heating of the A_M and H samples (H20 mainly) show a different behavior between 20 and 1250 °C. Within the range 20–900 °C this behavior is clearly due to the different crystalline phases in the original samples (Fig. 1). When the talc decomposes in A_M at above 1000 °C a different evolution of the crystalline phases can be observed, mainly in connection with the magnesium silicate phases. Besides, A_M seems to form some mullite as an intermediate product while in the H samples the spinel ($MgAl_2O_4$) is detected. At temperatures higher than 1300 °C all samples produce similar products.

Additionally, this reaction was followed by dilatometry (Figs. 6 and 7). In these figures, a systematic variation of the behavior with the milling time can be observed. The A_M sample does not present contraction between 20 and 500 °C, a zone where only gibbsite dehydration takes place. Later, it presents a contraction of three steps: a little one (575 °C peak), an intermediate one (975 °C peak) and the greater one at 1100 °C (Fig. 5). The two first steps are associated with the DTA peaks coming from kaolinite and talc. The last step in the 1150–1260 °C zone is associated with the sintering and the reaction to form new phases. The H samples show important differences, having a contraction from around 100 °C, becoming more intense with the increase of the milling time. Besides, the steps change, for instance, the one centered at 575 °C tends to disappear and it becomes unified in a continuous line from 20 to 800 °C for H20. The other two steps have also systematic changes, the H5 has two steps corresponding to 900 and 1120 °C peaks, respectively, the greater the one at 900°. The H10–H20 samples show a great step that corresponds to the 900° peak, followed by a slow contraction zone that has not peaks (Fig. 6).

All curves present a minimum from which they start to expand. This minimum tends to decrease with milling, starting from 1200° for A_M and reaching 1125° for H20. From this minimum, there is expansion of the materials and it corresponds to the dilation of the cordierite phases formed. In H20, it is possible to see the peak corresponding to the dilation beginning in Fig. 6.

The maximum contraction value increases with the milling, being the minimum for A_M (4.75%) and the maximum for H20 (16.2%). The main variations take place at times smaller than H10, as the H10–H20 samples present little change. Besides, the additional contraction of the H samples occurs mainly between 20 and 500° where A_M remains constant. It is interesting to observe that the final density reached in the five samples is similar. The greater

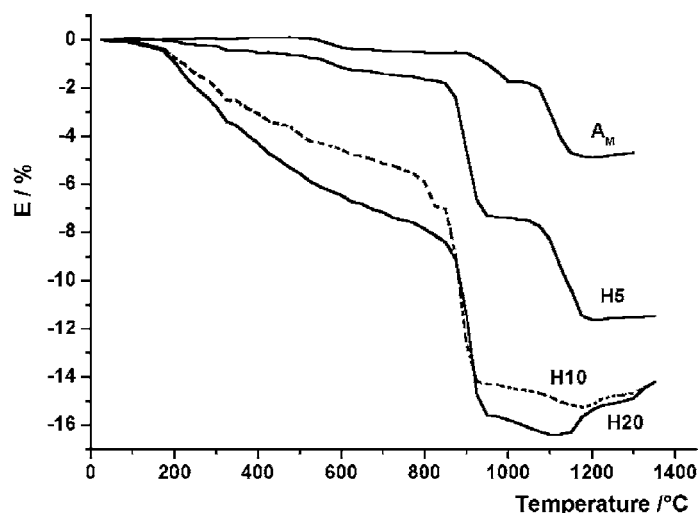


Fig. 6. Dilatometric curves for the minerals mixtures.

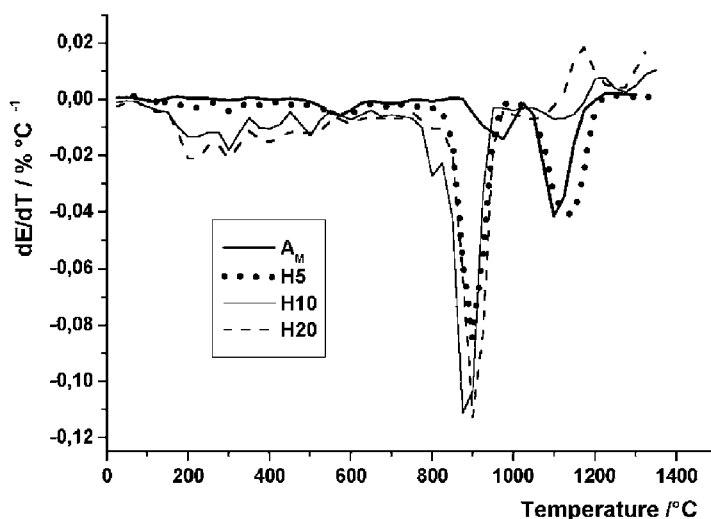


Fig. 7. Dilatometric derivative curves for the minerals mixtures.

contraction observed in Fig. 6 corresponds to a decrease of the green density with the increase of milling time.

Finally, some calcination experiences have been performed at different temperatures but with variable soaking time at those temperatures. At 900 °C, the A_M samples generate a totally amorphous product, while the H samples begin to form considerable amounts of clinoenstatite (MgO·SiO₂), as well as other magnesium silicates and spinel. The presence of magnesium phases increases with the increase of the milling time.

Within the range 100–1150 °C, the A_M and H samples present XRD clearly different as regards the content and type of magnesium crystalline phases present. At 1215 °C, the A_M as well as the H_X samples form cordierite but with a different relation with the intensity of the XRD peaks, which indicates a different growth of the crystalline planes. At 1350 °C, all samples generate similar final products as regards their crystalline phases such as cordierite and traces

of mullite and magnesium silicates. The differences in the cordierite formation for the H20 and A_M samples are within the range 1200–1300 °C.

4. Conclusions

The kaolinite, talc and gibbsite mixtures that generate cordierite are easily activated by milling. Due to the milling, to the minerals producing the crystalline structure loss and the reactivity increase. The mineral mixtures underwent mechanochemical effects that have been analyzed.

The DTA–TG and dilatometry techniques clearly indicate the structural modifications produced by milling on the kaolinite, gibbsite and talc. The mixture treated generates cordierite as the equilibrium phase at lower temperatures.

The greater differences in the cordierite formation are due to the different reaction mechanisms, which explains

the intermediate phases formed in the amorphized mixtures (H5–H20) and the reference samples (A–A_M). The main difference observed in the reaction mechanism was in connection with the magnesium silicate phases.

Acknowledgements

The authors wish to thank María Eugenia Ghirimoldi and Jorge Rinaldi for their contribution to this work.

References

- [1] P. Grosjean, *Cordierite Ceramics Interceram*. 42 (1993) 11–15.
- [2] K. Umehara, *Ceramic Honeycomb: After Treatment Technologies for Diesel Emissions*, NGK Insulators, Ltd., Japan, 1995, pp. 1–14.
- [3] C.A. Sorrell, *J. Am. Ceram. Soc.* 43 (7) (1960) 337–343.
- [4] A.D. Mazzoni, E.F. Aglietti, E. Pereira, *Latin Am. Res.* 21 (1991) 63–68.
- [5] V. Mingelgrin, L. Kliger, M. Gal, S. Saltzman, *Clays and Clay Miner.* 26 (4) (1978) 299–307.
- [6] E.F. Aglietti, J.M. Porto López, E. Pereira, *Int. J. Miner. Proc.* 16 (1986) 125–133.
- [7] E.F. Aglietti, J.M. Porto López, E. Pereira, *Int. J. Miner. Proc.* 16 (1986) 135–146.
- [8] J.G. Miller, T.D. Oulton, *Clays and Clay Miner.* 18 (6) (1970) 313–323.
- [9] E.F. Aglietti, A.N. Scian, M. Sacchi, J.M. Porto López, E. Pereira, *Latin Am. Chem. Eng. Appl. Chem.* 16 (1986) 33–43.
- [10] E.F. Aglietti, J.M. Porto Lopez, *Mater. Res. Bull.* 27 (1992) 1205–1216.
- [11] J. Temuujin, K. Okadaa, K.J.D. MacKenzie, *J. Eur. Ceram. Soc.* 18 (1998) 831–835.
- [12] J. Temuujin, K.J. MacKenzie, M. Schmucler, H. Schneider, J. McManus, S. Wimperis, *J. Eur. Ceram. Soc.* 20 (2000) 413–421.
- [13] A.D. Mazzoni, E.F. Aglietti, E. Pereira, *Latin Am. Res.* 21 (1991) 63–68.
- [14] E.T. Devyatkina, E.G. Avvakumov, N.V. Kosova, N.Z. Lyakhov, *Inorg. Mater.* 30 (1998) 227–229.
- [15] E.G. Avvakumov, M. Senna, N.V. Kosova, *Soft Mechanochemical Synthesis*, Kluwer Academic Publishers, Dordrecht, 2001 (Chapter 7).
- [16] S. De Aza, E. Monteros, *Bol. Soc. Esp. Ceram. Vidr.* 11 (1972) 315–321.